Complete Crystal Structure of Monocyte Chemotactic Protein-2, a CC Chemokine that Interacts with Multiple Receptors[†,‡]

Jaroslaw Blaszczyk,[§] Els Van Coillie,[||] Paul Proost,[||] Jo Van Damme,[||] Ghislain Opdenakker,[||] Grzegorz D. Bujacz,[⊥] Ji Ming Wang,[#] and Xinhua Ji*[,§]

Program in Structural Biology and Laboratory of Molecular Immunoregulation, National Cancer Institute, Frederick, Maryland 21702, USA, Rega Institute for Medical Research, Laboratory of Molecular Immunology, University of Leuven, Minderbroedersstraat 10, B-3000 Leuven, Belgium, and Technical University of Lodz, Institute of Technical Biochemistry, Stefanowskiego 4/10, 90-924 Lodz, Poland

Received April 25, 2000; Revised Manuscript Received September 8, 2000

ABSTRACT: Monocyte chemotactic protein 2 (MCP-2) is a CC chemokine that utilizes multiple cellular receptors to attract and activate human leukocytes. MCP-2 is a potent inhibitor of HIV-1 by virtue of its high-affinity binding to the receptor CCR5, one of the major coreceptors for HIV-1. Although a few structures of CC chemokines have been reported, none of these was determined with the N-terminal pyroglutamic acid residue (pGlu1) and a complete C-terminus. pGlu1 is essential for the chemotactic activity of MCP-2. Recombinant MCP-2 has Gln1 at the N terminus, 12−15% of which cyclizes automatically and forms pGlu1. The chemotactic activity of such MCP-2 mixture, which contains 12−15% pGlu1-form and 85−88% Gln1-form protein, is ∼10 times lower when compared with that of fully cyclized MCP-2 preparation. Therefore, this chemokine is practically inactive without pGlu1. We have determined the complete crystal structure of MCP-2 that contains both pGlu1 and an intact C-terminus. With the existence of pGlu1, the conformation of the N-terminus allows two additional interactions between the two subunits of MCP-2 dimer: a hydrogen bond between pGlu1 and Asn17 and a salt bridge between Asp3 and Arg18. Consequently, both pGlu1 are anchored and buried, and thereby, both N-terminal regions are protected against protease degradation. We have also observed not previously reported extended helical nature of the C terminal region, which covers residues 58−74.

Chemokines are important mediators of inflammatory and immunological responses. On the basis of the positions of first two cysteine residues, most chemokines belong to either the CXC or CC subfamily (*1*−*3*). Although the major biological function of chemokines is believed to be their capacity to induce leukocyte migration and activation, accumulating evidence suggests critical roles of chemokines in development, hematopoiesis, lymphocyte trafficking and homing, angiogenesis, and malignancy. Chemokines bind and activate seven transmembrane G protein-coupled cell surface receptors, some of which, CCR5 and CXCR4 in particular, are major coreceptors used by HIV-1 to enter and infect human cells (*4*, *5*). Therefore, the cognate chemokine ligands for CCR5 and CXCR4 are host derived anti-HIV-1 proteins by competitively occupying the HIV-1 coreceptors. Monocyte chemotactic protein 2 (MCP-2)[1] is a member of the CC chemokine subfamily copurified with MCP-1 and MCP-3 from human osteosarcoma and mononuclear cell supernatants (*6*). MCP-2 shares ∼60% amino acid identity with MCP-1 and MCP-3, and ∼30% identity with other CC chemokines such as MIP-1α, MIP-1*β*, and RANTES. Because of its capacity to interact with multiple receptors, MCP-2 chemoattracts and activates a variety of leukocyte populations. In addition to sharing CCR1 with MIP-1α, RANTES and MCP-3, and CCR2b with MCP-1 and MCP-3, MCP-2 binds and activates CCR5 (*7*). Therefore, like other CCR5 ligands such as MIP-1α, MIP-1*β*, and RANTES, MCP-2 is also a potent inhibitor of HIV-1 strains that use CCR5 as a coreceptor.

The structures of several CXC (*8*−*15*) and CC (*16*−*22*) chemokines have been solved. The common features of CXC and CC chemokines include a central three-stranded antiparallel *β*-sheet, an overlying C-terminal α-helix, and two disulfide bridges (Figure 1). Although the structures of MCP-1 (*17*, *19*) and MCP-3 (*20*, *23*) have been reported, none of these was determined with the N-terminal pyroglutamic acid residue (pGlu1) and with a complete C-terminus.

The pGlu1 residue has been postulated to be essential to the conformation of the N-terminus and the biological activity

[†] This work was supported in part by the Fund for Scientific Research of Flanders (FWO-Vlaanderen) and the Cancer Foundation of FB Verzekeringen NV, Belgium (J.V.D. and G.O.). P.P. holds a fellowship of the FWO-Vlaanderen, and E.V.C. is a postdoctoral fellow of the University of Leuven, Geconcerteerde OnderzoeksActies.

[‡] The atomic coordinates and structure factors have been deposited in the PDB as entry 1ESR.

* To whom correspondence should be addressed. Phone: (301) 846-5035. Fax: (301) 846-6073. E-mail: jix@ncifcrf.gov. Postal: NCI at Frederick, Building 539, Room 124, P.O. Box B, Frederick, MD 21702-1201, USA.

[§,#] National Cancer Institute at Frederick, USA.

[||] University of Leuven, Belgium.

[⊥] Technical University of Lodz, Poland.

[1] Abbreviations: MCP, monocyte chemotactic protein; MIP, macrophage inflammatory protein; RANTES, regulated on activation normal T-cell expressed and secreted; AOP-RANTES, a chemically modified aminooxypentane derivative of RANTES; pGlu, pyroglutamic acid; rms, root-mean-square; PDB, Protein Data Bank.

10.1021/bi0009340 CCC: $19.00
Published on Web 10/24/2000

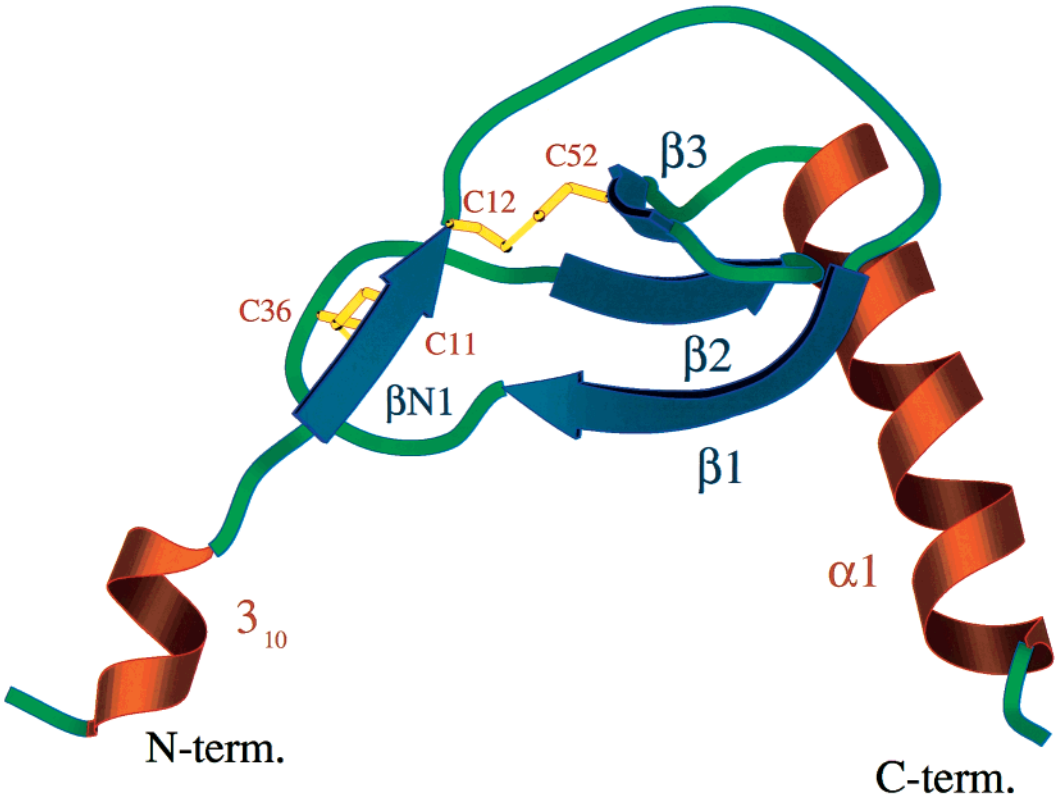

FIGURE 1: Architecture of MCP-2 monomer and secondary structure assignment. Helices are shown as orange spirals and β-strands are shown as blue arrows. Cysteine side chains and disulfide bonds are shown in yellow. The figure was made using BOBSCRIPT (*37*).

of MCP proteins. To address the biological significance of pGlu1 in MCP-2, we have cloned and expressed this chemokine with N-terminal Gln1 in *Escherichia coli*, purified the recombinant protein to homogeneity, and chemically converted Gln1 at the N-terminus into pGlu1 (*24*). We found that pGlu1 is essential for the chemotactic activity of MCP-2 and that it protects the N-terminal region against protease degradation (*24*).

EXPERIMENTAL PROCEDURES

Mass Spectrometry. Recombinant MCP-2 was expressed in *E. coli* and purified with HPLC as previously described (*24*). All mass spectra were measured on an Esquire LC/MS ion trap mass spectrometer (Bruker Daltonic, Bremen, Germany) with direct infusion of the diluted HPLC fractions (1/30 dilution in 1/1 acetonitrile/water containing 0.1% formic acid) at a flow rate of 5 μL/min. For the average of more than 100 spectra, the error on the relative molecular mass of a 10-kDa protein should be ~1 Da or smaller. Figure 2, panel a is the averaged profile spectrum (averages of 238 spectra). The deconvolution of the averaged profile spectrum (Figure 2, panel b) shows the relative molecular masses of both MCP-2 forms. The theoretical average relative molecular mass for MCP-2 with Gln1 at the N terminus is 8910.4, whereas it is 8893.3 for the protein with the N-terminal pGlu1. According to the peak intensities in Figure 2, panel b, 15% of the MCP-2 is spontaneously converted into the pGlu1-form. For a second preparation of recombinant MCP-2, 12% of the purified chemokines was spontaneously converted into the pGlu1-form (data not shown).

Crystallization and Data Collection. The chemical conversion of the recombinant MCP-2 was performed as previously described (*24*). Crystals of MCP-2 grew in hanging drops at well-controlled room temperature. The drops contained equal volumes of reservoir and protein stock solutions. The protein stock solution contained 3 mg/mL protein in 10 mM Tris-HCl (pH 8.0), and the reservoir solution contained 40% ammonium sulfate in 50 mM Tris-HCl (pH 7.5). The bipyramid hexagonal microcrystals appeared in 1 h, and they reached the final size (0.25 × 0.25 × 0.55 mm) in 2 weeks. The protein crystallized in hexagonal space group $P6_122$ with one MCP-2 molecule in the asymmetric unit and diffracted to 2.0-Å resolution. The unit cell dimensions were $a = b = 61.01$ Å and $c = 114.93$ Å. The solvent content of the crystals was 63%, and the Matthews number (V_m) was 3.6 Å^3/Da (Matthews, 1968). The data set was collected from a single crystal at 100 K with an ADSC Quantum4 CCD system mounted on synchrotron beamline X9B at the National Synchrotron Light Source in Brookhaven National Laboratory (Upton, NY). Mineral oil (Sigma M3516) was used as the cryoprotectant and suspension medium to mount the crystal in the cryo loop. Data processing was carried out with the HKL2000 suite (*25*). The data set consisted of 9060 unique reflections, within the resolution range of 20.0 to 2.0 Å, reduced from a total of 38 808 measurements and was 99.0% complete. The internal *R*-factor between symmetry-related reflections was 5.6% (Table 1).

Crystal Structure Determination and Refinement. The crystal structure of MCP-2 was solved by molecular replacement with the program AMoRe (*26*). The search model was a single molecule of MCP-1 (*19*) without solvent. The solution from molecular replacement after rotation and translation search consisted of a single molecule and had a correlation coefficient of 0.53 and a crystallographic *R*-factor

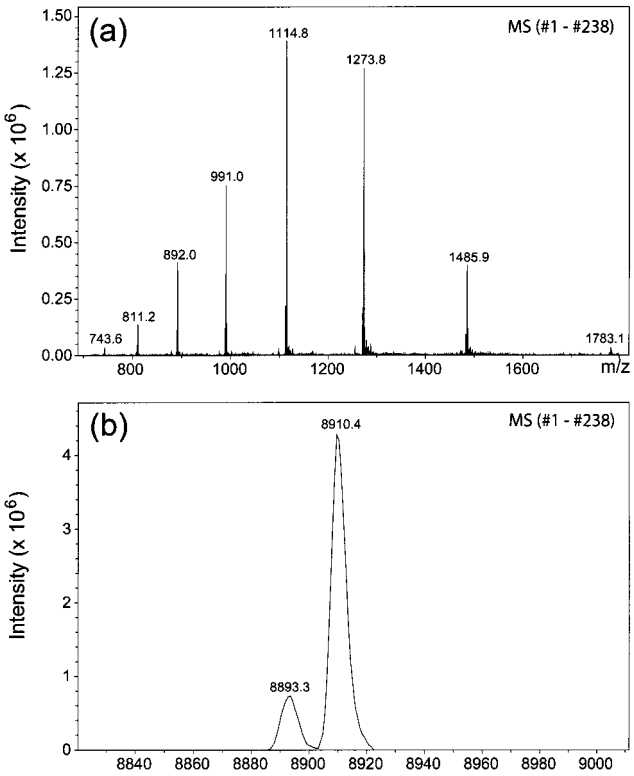

FIGURE 2: Mass spectra of MCP-2: (a) Recombinant protein purified by reversed phase HPLC was subjected to electrospray ion trap mass spectrometry. The averaged profile spectrum of 238 spectra is shown. (b) Deconvolution of the averaged profile spectrum (see panel a) shows the relative molecular masses of both MCP-2 forms. For a second preparation of recombinant MCP-2, 12% of the purified chemokines was spontaneously converted into the pGlu1 form (data not shown).

Table 1: Crystal Data and Experimental Details for Human MCP-2

crystal shape	hexagonal bipyramid
crystal dimensions (mm)	0.25 × 0.25 × 0.55
space group	$P6_122$
unit cell dimensions (Å)	$a = b = 61.01$, $c = 114.93$
molecules/asymmetric unit	1
solvent content (%)	63
matthews number (Å^3/Da)	3.6
X-ray source	X9B, NSLS, BNL
temperature (K)	100
resolution (Å)	2.0
observed reflections	38808
unique reflections	9060
overall completeness (%)	99.0
overall R_{sym} (%)	0.056
last shell[a] completeness (%)	97.6
last shell[a] R_{sym} (%)	0.390
last shell[a] $I/\sigma(I)$	3.4

[a] 2.03 to 2.00 Å.

of 0.43. The model of MCP-2, containing residues 2 to 71, was built and was initially refined with the program X-PLOR (*27*) against data in the resolution range 8.0 to 2.0 Å. The refinement was started with the rigid-body procedure and was continued using simulated annealing. After the first round of refinement, the $F_o - F_c$ map showed the density for pGlu1 and that for five residues at the C-terminus. Since the new density was not readily interpretable at this stage, the pGlu1 and five C-terminal residues were not built. The uncertain segments of the model were checked and adjusted with simulated annealed omit maps. Further model building was continued by the addition of water molecules and further adjustment of side chains that showed deviation from the electron density. After each round of refinement, the entire model was inspected with the $2F_o - F_c$ and $F_o - F_c$ maps. Water molecules with *B*-factors higher than 80 Å^2 were rejected. The refinement of the model with integrated water molecules clearly defined the position of the last five residues at the C terminus and the conformation of pGlu1. Final refinement was performed with the program SHELXL-97 (*28*), against all data within the resolution range of 20.0 to 2.0 Å, using the least-squares block-diagonal matrix technique. After the structure was completed, all water molecules were verified with a series of omit maps; ~30 water molecules were removed and verified each time. The model building and adjustment were carried out with the O graphics package (*29*). The final structure contains all non-hydrogen atoms of the full-length polypeptide chain and 89 water molecules. The model refinement and final statistics are summarized in Table 2.

Table 2: Summary of Human MCP-2 Structure Refinement

no. reflections for refinement/R_{free}	8555/471
no. least-squares parameters	2793
no. residues/(non-H) atoms	76/624
no. water oxygen atoms	89
final R_{free}/R for $I \geq 2\sigma(I)$	0.299/0.229
final R_{free}/R for all data	0.320/0.244
rms deviation from ideal geometry (Å)	
bond length	0.008
angle distance	0.029
estimated coordinate error (Å)[a]	0.22
average *B*-factor (Å^2)	
overall	49.2
main chain	41.7
side chain	53.4
water	59.8
Ramachandran plot statistics	
residues in most-favored regions	65 (95.6%)
residues in additional allowed regions	3 (4.4%)

[a] From Luzzati plot.

RESULTS AND DISCUSSION

Complete Structure of Human MCP-2. Human MCP-2 exists in two isoforms, MCP-2Lys$_{46}$ and MCP-2Gln$_{46}$, with identical patterns of receptor interaction and biological activity (*24*). We have determined the crystal structure of MCP-2Gln$_{46}$ that contains 76 amino acid residues and 89 water molecules at 2.0-Å resolution. The accuracy of the atomic positions versus the resolution derived from the Luzzati plot shows a coordinate error of ~0.22 Å. As indicated by the Ramachandran plot (*30*), all main-chain dihedral angles are found in favorable regions. All atoms are in good agreement with the final electron density contoured at 1.0 σ except for the side chains of Phe71 and Leu74 in the C-terminal region. All water molecules have densities above 1.0 σ in the final $2F_o - F_c$ map.

The architecture of the human MCP-2 monomer is similar to that of other previously reported CC chemokines, such as MCP-1 (*17*, *19*), MCP-3 (*20*), MIP-1β (*18*), RANTES (*16*, *21*, *22*), and eotaxin (*31*). The secondary structure elements of human MCP-2 are organized with the topology $\alpha 3_{10}-\beta N1-\beta 1-\beta 2-\beta 3-\alpha 1$ (Figure 1). Residues 3 to 7 in MCP-2 form a short $\alpha 3_{10}$-helix followed by an irregular βN1-strand (residues 9−11) that is linked to β1 via an extended loop

```
                10         20         30         40
huMCP-1    XPDAINAPVT CCYNFTNRKI SVQRLASYRR ITSSKCPKEA
huMCP-2    XPDSVSIPIT CCFNVINRKI PIQRLESYTR ITNIQCPKEA
huMCP-3    XPVGINTSTT CCYRFINKKI PKQRLESYRR TTSSHCPREA
huMCP-4    XPDALNVPST CCFTFSSKKI SLQRLKSY-V ITTSRCPQKA
huEotaxin  GPASV--PTT CCFNLANRKI PLQRLESYRR ITSGKCPQKA
huRANTES   SPYSSD-TTP CCFAYIARPL PRAHIKEYFY -TSGKCSNPA
huMIP-1α    SLAADTPTA CCFSYTSRQI PQNFIADYFE -TSSQCSKPG
huMIP-1β   APMGSDPPTA CCFSYTARKL PRNFVVDYYE -TSSLCSQPA

                50         60         70
huMCP-1    VIFKTIVAKE ICADPKQKWV QDSMDHLDKQ TQTPKT
huMCP-2    VIFKTQRGKE VCADPKERWV RDSMKHLDQI FQNLKP
huMCP-3    VIFKTKLDKE ICADPTQKWV QDFMKHLDKK TQTPKL
huMCP-4    VIFRTKLGKE ICADPKEKWV QNYMKHLGRK AHTLKT
huEotaxin  VIFKTKLAKD ICADPKKKWV QDSMKYLDQK SPTPKP
huRANTES   VVFVTRKNRQ VCANPEKKWV REYINSLEMS
huMIP-1α   VIFLTKRSRQ VCADPSEEWV QKYVSDLELS A
huMIP-1β   VVFQTKRSKQ VCADPSESWV QEYVYDLELN
```

FIGURE 3: Sequence alignment of human CC chemokines. Residues conserved in all four MCPs are shaded. The N-terminal residue, pGlu1, is marked with an "X". The amino acid sequence identity of MCP-2 is 62% with MCP-1, 57% with MCP-3, and 55% with MCP-4. The highest sequence identity among CC chemokines is 71% between MCP-1 and MCP-3.

(residues 12−24). β1 (residues 25−31), β2 (residues 40−45), and β3 (residues 50−53) fold into a three-stranded antiparallel β-sheet, which is part of a Greek key motif and is followed by the C-terminal helix α1 (residues 58−74). Two disulfide bridges between four cysteine residues (Figure 3) show a left-handed spiral conformation (Figure 1). The first bridge, Cys11−Cys36, couples βN1 with the hairpin loop between β1 and β2, and the second one, Cys12−Cys52, connects βN1 and β3 (Figure 1). Therefore, the disulfide bonds, as in other CC chemokines, play an important role in stabilizing the β-structure of MCP-2. The stabilization of the MCP-2 β-structure is also assisted by the side chain of Gln46, which forms hydrogen bonds with the carbonyl oxygen of Gln23 and with NH1 of Arg24. Gln46 is located in the turn between β2 and β3, whereas Gln23 and Arg24 are at the beginning of β1. Similar interactions can be predicted for MCP-2Lys$_{46}$, where Lys46 should be able to form a hydrogen bond with Gln23, although the interaction between Lys46 and Arg24 is not favorable. This finding is consistent with the results of biological assays, which have demonstrated that the two variants of human MCP-2 do not differ significantly in their function (*24*).

pGlu1 is Essential for the Chemotactic Activity of MCP-2. We have previously demonstrated that the chemotactic activity of the recombinant MCP-2 with N-terminal Gln1 is 10 times lower than that of the pGlu1 version (*24*). In this study, we have established that before the chemical conversion of Gln1 to pGlu1, there is 85−88% Gln1-form and 12−15% pGlu1-form in the recombinant protein (Figure 2), indicating that 12−15% of the Gln1 cyclizes automatically and form pGlu1, which is consistent with the 10-fold lower chemotactic activity when compared with 100% cyclized MCP-2. We therefore conclude that pGlu1 is essential for the chemotactic activity of MCP-2 and that this chemokine is practically inactive without it.

The N-terminal pGlu1 is essential for the biological activity of many proteins such as peptide hormones thyrotropin-releasing hormone (*32*, *33*), luteinizing hormone-releasing hormone (*34*), and a cytotoxic ribonuclease onconase (*35*, *36*). The roles of pGlu1 have been proposed to form a hydrogen bond with C-terminal residues or participate in substrate binding. For instance, the N- and C-termini of luteinizing hormone-releasing hormone interact with each other via the formation of a hydrogen bond between the pyrrolidone carbonyl group of pGlu1 and the glycinamide group (*34*). Such interaction is critical for the formation of receptor binding conformation of the hormone. In onconase, pGlu1 not only forms a hydrogen bond with Val96 in the C-terminal β-sheet but is also part of the active site for substrate binding (*36*). A recombinant onconase with an N-terminal methionine (Met0) proceeding Gln1 showed decreased cytotoxicity and enzymatic activity, while cleavage of Met0 and cyclizing Gln1 to reform pGlu1 reconstituted the cytotoxicity and ribonucleolytic activity of this enzyme (*35*).

pGlu1 of MCP-2 is Essential to the Conformation of N-Terminus. The N- and C-termini are far apart in a single molecule of MCP-2 (Figure 1). Therefore, pGlu1 cannot form a hydrogen bond with a C-terminal residue as observed for onconase where pGlu1 folds back against the N-terminal α-helix (*36*). In MCP-2, pGlu1 points forward such that its pyrrolidone carbonyl group points to the same direction as the carboxylic side chain of Asp3. Thus in dimeric MCP-2, the N-terminus of one subunit is able to form a hydrogen bond and a salt bridge with residues in the loop following βN1 in the other subunit (Figure 4, panel a, and Figure 5, panel a, this work), in addition to an identical set of six hydrogen bonds between the two subunits previously reported for MCP-1 (*19*). Four of these six hydrogen bonds are between the main-chain atoms of Ile9 and Cys11 on both βN1-strands, of which the average distance is ~3.0 Å (Figure 4, panel b). The fifth hydrogen bond is between the hydroxyl groups of Thr10 from both monomers with a distance of 2.65 Å (Figure 4, panel b), and the sixth is between the carbonyl oxygen atom of Ser6 and the amide nitrogen atom of Cys52 (not shown for clarity). Furthermore, a water molecule is present within the hydrogen bond distance to the carbonyl oxygen of Ile9 and the amide nitrogen of Cys11 in both subunits (Figure 4, panel b). Although the water-bridged interactions have also been reported for MCP-1 (*19*), the two interactions involving pGlu1 and Asp3 in one subunit with Asn17 and Arg18 in the other have not been observed in any other MCP structures, in which pGlu1 is either absent or replaced with Gln1.

Figure 5, panel a, schematically represents the MCP-2 dimer showing the secondary-structure features and Figure 5, panel b, illustrates the alignment of three MCP dimers derived from their crystal structures, including MCP-2 (this work) and the I-form[2] (with a monomer in the asymmetric unit) and P-form (with a dimer in the asymmetric unit) MCP-1 (*19*). Unlike the MCP-2 structure, both MCP-1 structures were determined with N-terminal Gln1. The superposition was done via optimizing the alignment of one subunit. Although in general, MCP-2 is very similar to the P-form MCP-1 and less similar to the I-form, striking conformational differences have been revealed at the N-termini between the three MCPs. The N-termini of MCP-1 do not have a unique conformation, as evidenced by the

[2] The I-form of MCP-1 contains a monomer in the asymmetric unit, and the P-form has a dimer in the asymmetric unit.

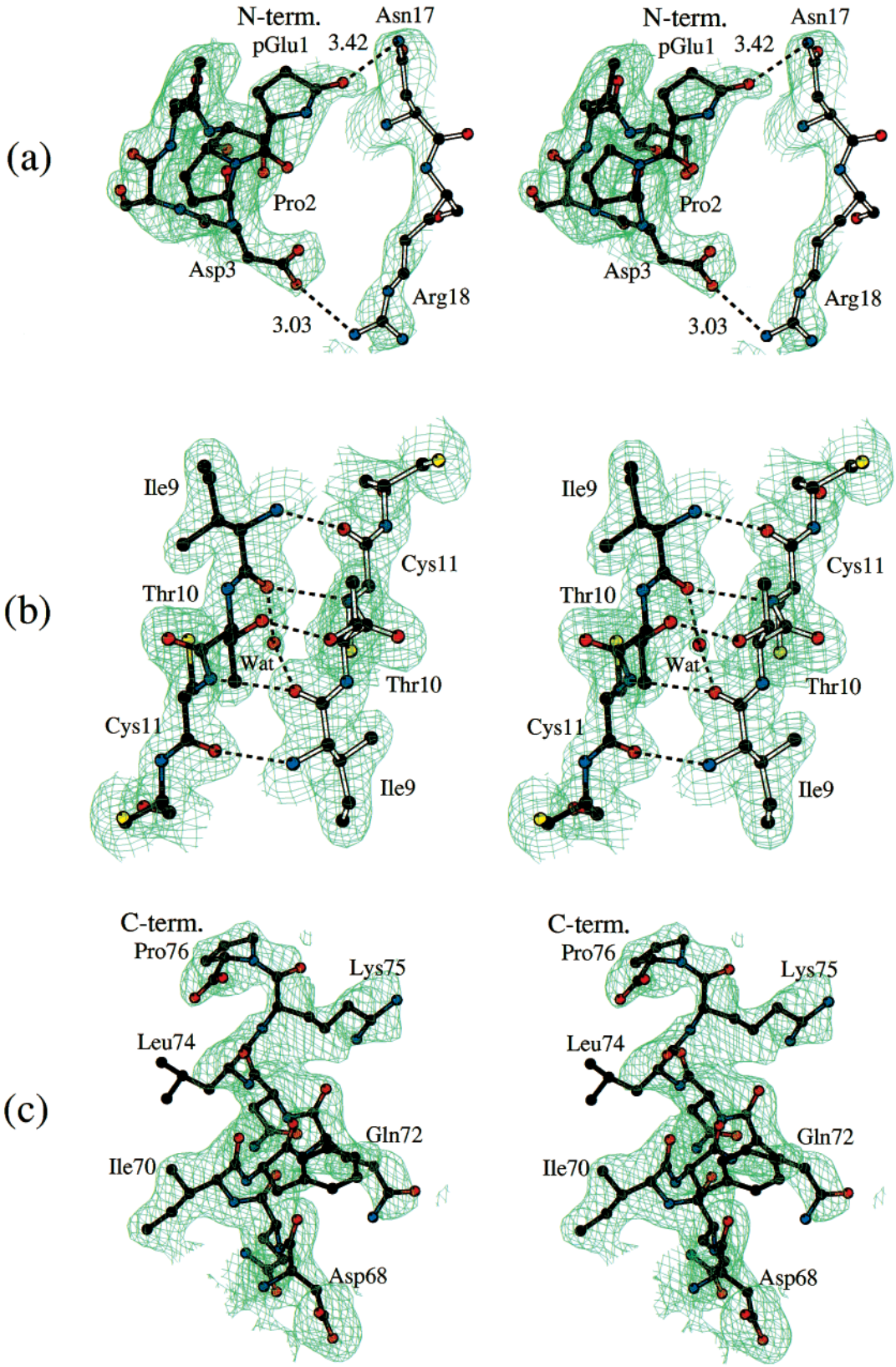

FIGURE 4: Final model of MCP-2 dimer with 2*Fo* − *Fc* electron density map contoured at 1.0 σ. The two subunits are distinguished with "filled" and "open" bonds. The electron density map is illustrated as a green net. The dotted lines represent hydrogen bonds and salt bridges. (a) The N-terminal residues from pGlu1 to Ser6 of one subunit interact with residues Asn17 and Arg18 from the other subunit. (b) Part of the subunit-subunit interaction involves residues 9 to 11 from both subunits and a water molecule shared by the two subunits. (c) The structure of C-terminal residues from Asp68 to Pro76 illustrates that the C-terminal helix of MCP-2 extends to Leu74. The figures were made using BOBSCRIPT (*37*).

different conformation of the I-form and P-form protein. However, the N-termini of both I- and P-form MCP-1 point away from the loop following βN1 of the other subunit (Figure 5, panel b). In contrast, the N-terminal regions of

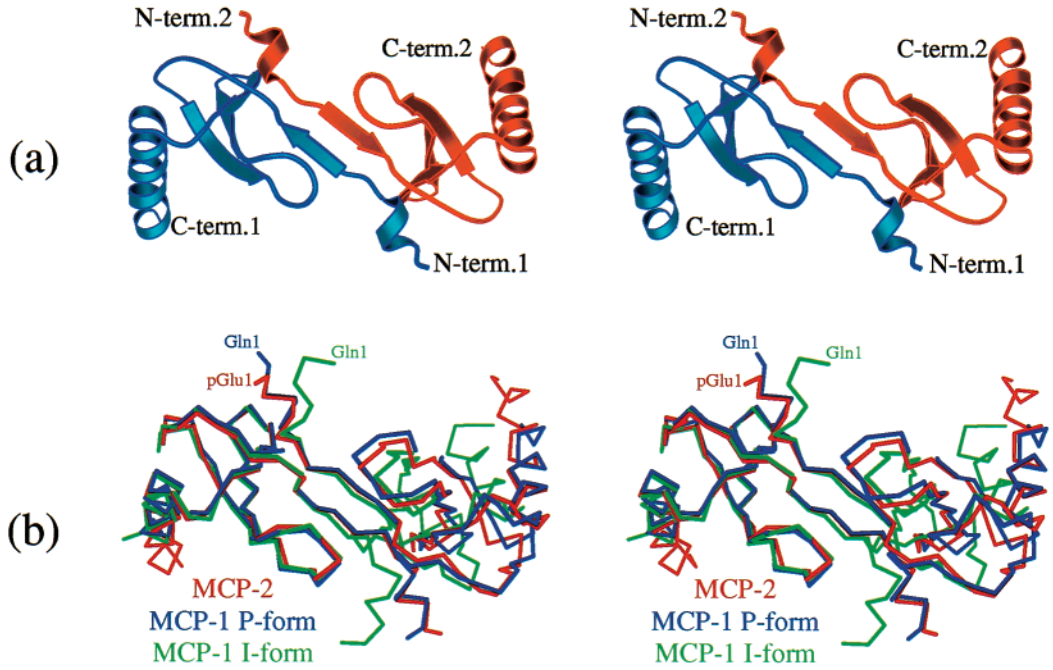

FIGURE 5: Putative dimers of chemokines. (a) Stereoview of the MCP-2 dimer showing the secondary structure features. The two subunits are distinguished with two colors. The N- and C-termini are labeled. (b) Stereoview showing the superimposed crystal structures of MCP dimers, including MCP-2 (red) and the I- (green) and P-form (violet) MCP-1 (*19*). Superposition is made on the basis of one subunit to illustrate the conformational difference at the N-termini as well as the variability of the dimers. The figures were made using BOBSCRIPT (*37*).

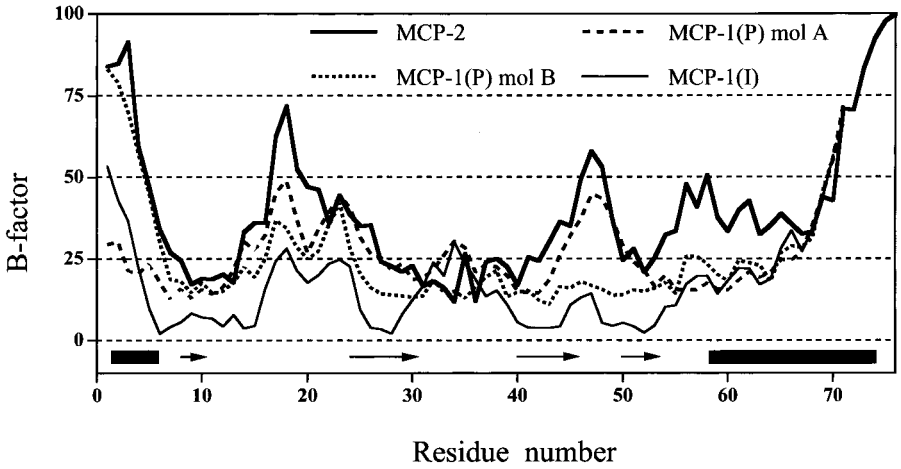

FIGURE 6: Main-chain atomic temperature factors (*B*-factors) of MCP-2 (this work) and two forms of MCP-1 (*19*). In addition to the N- and C-termini, two regions of MCP-2 (residues 15−24 and 46−50) display increased mobility. The arrows denote β-strands, and helical regions are marked as bars.

MCP-2 dimer are anchored to the loops following the βN1 strands. Therefore, we conclude that pGlu1 is essential to the conformation of N terminus, which allows the N-terminal interaction with the other subunit, and thus, both N-terminal regions are protected against protease degradation.

Mobility of the Polypeptide Chain and C-Terminal Helix. Our MCP-2 structure provides the first complete structure of any MCP protein with its native pGlu1 at the N-terminus and a 4.5-turn helix at the C-terminus (Figures 1 and 4). The mobility of a polypeptide chain can be indicated by the *B*-factors of the main chain atoms (Figure 6). MCP-2 has increased mobility in both the N- and C-terminal regions. In addition, two regions, residues 15−24 and 46−50, display higher-than-average mobility. The first region is the loop between βN1 and β1, and the second region is the turn between β2 and β3. The higher-than-average mobility in region 15−24 is correlated with an even higher mobility of the N-terminal region because the N-terminus is anchored to this loop (region 15−24, Figure 4, panel a, and Figure 5). Such correlation is not observed for MCP-1 because the N-terminus points away from the loop following βN1 (Figure 5, panel b, and Figure 6). The mobility in region 46−50 propagates into the C-terminal helix, of which the last helical turn (region 71−74) and residues Lys75 and Pro76 show the highest mobility (Figure 6). The side chain of Lys75 has multiple conformations and those of Phe71 and Leu74 are not well-defined (Figure 4, panel c), most likely because the C-terminal region of MCP-2 is not involved in intermolecular interactions. In the crystal structures of MCP-1, the last five residues at the C-terminus of P-form and the last six residues at the C-terminus of I-form are missing (*19*). The NMR structures of MCP-1 (*17*) and MCP-3 (*20*, *23*) did not show

the helical nature of region 71−74. Although the C-terminal structure has previously been determined for AOP-RANTES (*16*, *21*, *22*) and MIP-1β (*18*), the C-terminus in these two proteins is six residues shorter than that of MCPs (Figure 3) and, therefore, has only three turns. The three-turn C-terminal helix of AOP-RANTES has been observed in both crystal (*22*) and NMR (*16*, *21*) structures and that of MIP-1β has been defined by NMR only (*18*). Therefore, it is evident that the C-terminus of CC chemokines is completely helical, an observation that may be functionally important.

pGlu1, Dimerization, and N-Terminal Protection in MCP-2. The crystal structure of MCP-2 reveals a "four-legged" architecture (Figure 5, panel a). Two of the four legs are the negatively charged C-termini. The side chains of Gln23, Arg24, Gln46, and Arg47 in the two subunits form another two legs. Because the two variants of MCP-2Lys$_{46}$ and MCP-2Gln$_{46}$ use same receptors and exhibit identical biological activity (*24*), the number of charges on these two legs may not necessarily be important for their function. Although the physiological significance of this four-legged architecture remains unresolved, our dimeric structure does shed light on the protease stability of MCP-2. We have previously demonstrated that N-terminal pGlu1 protects the N terminal region against degradation by CD26/dipeptidyl peptidase IV, an aminopeptidase able to cleave Pro−Xaa bonds (*24*). The crystal structures of MCP-2 (this work) and MCP-1 (*19*) suggest that with pGlu1, the N-termini of dimeric MCP are involved in subunit−subunit interactions (Figure 4, panel a, and Figure 5) and therefore are buried and protected against the protease cleavage and that the N-terminus of Gln1-form MCP does not interact with the other subunit (Figure 5, panel b) and therefore is exposed and not protected.

ACKNOWLEDGMENT

We thank Dr. Z. Dauter for his kind help during data collection and processing at the National Synchrotron Light Source, Brookhaven National Laboratory, Dr. I. Van Aelst for providing technical assistance, and Dr. A. Wlodawer for critical reading of the manuscript. J.B. also thanks Prof. M. W. Wieczorek, Technical University of Lodz, Poland, for continuous encouragement.

REFERENCES

1. Baggiolini, M., Dewald, B., and Moser, B. (1994) *Adv. Immunol. 55*, 97−179.
2. Oppenheim, J. J., Zachariae, C. O., Mukaida, N., and Matsushima, K. (1991) *Annu. Rev. Immunol. 9*, 617−648.
3. Luster, A. D. (1998) *N. Engl. J. Med. 338*, 436−445.
4. D′Souza, M. P., and Harden, V. A. (1996) *Nat. Med. 2*, 1293−1300.
5. Premack, B. A., and Schall, T. J. (1996) *Nat. Med. 2*, 1174−1178.
6. Van Damme, J., Proost, P., Lenaerts, J. P., and Opdenakker, G. (1992) *J. Exp. Med. 176*, 59−65.
7. Gong, W., Howard, O. M., Turpin, J. A., Grimm, M. C., Ueda, H., Gray, P. W., Raport, C. J., Oppenheim, J. J., and Wang, J. M. (1998) *J. Biol. Chem. 273*, 4289−4292.
8. Baldwin, E. T., Weber, I. T., St. Charles, R., Xuan, J. C., Appella, E., Yamada, M., Matsushima, K., Edwards, B. F., Clore, G. M., Gronenborn, A. M., and Wlodawer, A. (1991) *Proc. Natl. Acad. Sci. U.S.A. 88*, 502−506.
9. Clore, G. M., Appella, E., Yamada, M., Matsushima, K., and Gronenborn, A. M. (1990) *Biochemistry 29*, 1689−1696.
10. Clore, G. M., and Gronenborn, A. M. (1991) *J. Mol. Biol. 217*, 611−620.
11. Fairbrother, W. J., Reilly, D., Colby, T. J., Hesselgesser, J., and Horuk, R. (1994) *J. Mol. Biol. 242*, 252−270.
12. Kim, K. S., Clark-Lewis, I., and Sykes, B. D. (1994) *J. Biol. Chem. 269*, 32909−32915.
13. Malkowski, M. G., Wu, J. Y., Lazar, J. B., Johnson, P. H., and Edwards, B. F. (1995) *J. Biol. Chem. 270*, 7077−7087.
14. St. Charles, R., Walz, D. A., and Edwards, B. F. (1989) *J. Biol. Chem. 264*, 2092−2099.
15. Zhang, X., Chen, L., Bancroft, D. P., Lai, C. K., and Maione, T. E. (1994) *Biochemistry 33*, 8361−8366.
16. Chung, C. W., Cooke, R. M., Proudfoot, A. E., and Wells, T. N. (1995) *Biochemistry 34*, 9307−9314.
17. Handel, T. M., and Domaille, P. J. (1996) *Biochemistry 35*, 6569−6584.
18. Lodi, P. J., Garrett, D. S., Kuszewski, J., Tsang, M. L., Weatherbee, J. A., Leonard, W. J., Gronenborn, A. M., and Clore, G. M. (1994) *Science 263*, 1762−1767.
19. Lubkowski, J., Bujacz, G., Boque, L., Domaille, P. J., Handel, T. M., and Wlodawer, A. (1997) *Nat. Struct. Biol. 4*, 64−69.
20. Meunier, S., Bernassau, J. M., Guillemot, J. C., Ferrara, P., and Darbon, H. (1997) *Biochemistry 36*, 4412−4422.
21. Skelton, N. J., Aspiras, F., Ogez, J., and Schall, T. J. (1995) *Biochemistry 34*, 5329−5342.
22. Wilken, J., Hoover, D., Thompson, D. A., Barlow, P. N., McSparron, H., Picard, L., Wlodawer, A., Lubkowski, J., and Kent, S. B. (1999) *Chem. Biol. 6*, 43−51.
23. Kim, K. S., Rajarathnam, K., Clark-Lewis, I., and Sykes, B. D. (1996) *FEBS Lett. 395*, 277−282.
24. Van Coillie, E., Proost, P., Van Aelst, I., Struyf, S., Polfliet, M., De Meester, I., Harvey, D. J., Van Damme, J., and Opdenakker, G. (1998) *Biochemistry 37*, 12672−12680.
25. Otwinowski, Z., and Minor, W. (1997) *Methods Enzymol. 276*, 307−326.
26. Navaza, J. (1994) *Acta Crystallogr. A 50*, 157−163.
27. Brünger, A. T., and Rice, L. M. (1997) *Methods Enzymol. 277*, 243−269.
28. Sheldrick, G. M., and Schneider, T. R. (1997) *Methods Enzymol. 277*, 319−343.
29. Jones, T. A., and Kjeldgaard, M. (1997) *Methods Enzymol. 277*, 173−208.
30. Laskowski, R. A., MacArthur, M. W., Moss, D. S., and Thornton, J. M. (1993) *J. Appl. Crystallogr. 26*, 283−291.
31. Crump, M. P., Rajarathnam, K., Kim, K. S., Clark-Lewis, I., and Sykes, B. D. (1998) *J. Biol. Chem. 273*, 22471−22479.
32. Folkers, K., Chang, J. K., Currie, B. L., Bowers, C. Y., Weil, A., and Schally, A. V. (1970) *Biochem. Biophys. Res. Commun. 39*, 110−113.
33. Hinkle, P. M., Woroch, E. L., and Tashjian, A. H., Jr. (1974) *J. Biol. Chem. 249*, 3085−3090.
34. Seprodi, J., Coy, D. H., Vilchez-Martinez, J. A., Pedroza, E., Huang, W. Y., and Schally, A. V. (1978) *J. Med. Chem. 21*, 993−995.
35. Boix, E., Wu, Y., Vasandani, V. M., Saxena, S. K., Ardelt, W., Ladner, J., and Youle, R. J. (1996) *J. Mol. Biol. 257*, 992−1007.
36. Mosimann, S. C., Ardelt, W., and James, M. N. (1994) *J. Mol. Biol. 236*, 1141−1153.
37. Esnouf, R. M. (1997) *J. Mol. Graph. Model. 15*, 132−134, 112−113.
38. Nicholls, A., Sharp, K. A., and Honig, B. (1991) *Proteins: Struct. Funct. Genet. 11*, 281−296.

BI0009340